Investigation of Tetramethylenesulfonated Calix[4]resorcinarene Interactions with Azo Dyes in Aqueous Solution

Julia E. Morozova, Ella Kh. Kazakova,* Diana A. Mironova, Yana V. Shalaeva, Victor V. Syakaev, Nely A. Makarova, and Alexander I. Konovalov

A. E. Arbuzov Institute of Organic and Physical Chemistry of Kazan Scientific Center of Russian Academy of Sciences, Arbuzov Street 8, Kazan, 420088 Russian Federation

Received: July 1, 2010; Revised Manuscript Received: August 27, 2010

The interaction of a macrocycle's aggregates with a guest molecule has special interest due to the double role, both of macrocycle cavity and self-associates, in the binding of the guests. Here, we report on the interactions of nonaggregated methyl-substituted (SCA1) and aggregated penthyl-substituted (SCA2) tetramethylenesulfonated calix[4]resorcinarenes with pH indicators methyl yellow (MY) and methyl orange (MO) in aqueous solutions. It was found that the pH of aqueous solutions of SCA1 and SCA2 depends on their concentration; besides, variation of the concentration of SCA1 and SCA2 results in a shift of the absorption maxima and of pH-sensitive azo dyes. Association of the marocycles with azo dyes was demonstrated to follow a proton-transfer mechanism accompanied by protonation of the dyes; it was found that excess of the macrocycle in solution with the universal buffer background shifts the pK_a values and stabilizes the protonated form of the dyes. Consideration of interactions of small dye molecules with large molecular associates, containing both individual and multimolecule binding sites, gives a closer approximation of synthetic biomimetics to their natural prototypes.

Introduction

Investigation of the binding properties of water-soluble tetramethylenesulfonated calixarenes, once touching their amphiphilic long-chain derivatives ($\geq C_5H_{11}$), inevitably has to deal with their surfactant properties. Indeed, the presence of at least four substituents of C_5H_{11} or greater length results in a macrocycle with properties similar to those of surfactants with $C_{17}-C_{18}$ long chains and a hydrophilic sulfate or sulfonate head (CMC of calixarene = 0.89 mM, $N_{agr} = 3$;[1,2] CMC of lauryl sulfate = 8.2 mM, $N_{agr} = 62$[3]). Even in millimolar concentrations, typically used to study the binding properties of host molecules by physical and physicochemical methods, such macrocycles in aqueous solution exist as associates. Dilution aimed at dissociating these aggregates results in solutions of concentrations too low for both NMR and UV−vis spectroscopy. On the other hand, aggregation of the macrocycles enables the study of their truly supramolecular binding properties and estimation of the impact of self-association. Even a simple comparison of the binding properties of C_5H_{11}- and CH_3-substituted calixarenes with the same guests provides impressive insight into this insufficiently explored aspect of supramolecular chemistry.

Most literature data on calixarene interactions with dyes deal with 1:1 complexes;[4−10] only a small number of papers actually describe the interactions of dyes with micellar solutions of calixarenes.[6,11,12] The authors of the ref 6 described the solubilizaton of water-insoluble azo dyes Orange OT, MY, Sudan III, and *p*-hydroxyazobenzene by sulfonatocalix[*n*]arenas (n = 6, 8) forming inclusion 1:1 host−guest complexes. Interaction of acid−base indicators with micellar solutions of calixarenes in aqueous media is accompanied with certain changes in their protolytic properties, similar to those observed for their associates with surfactants.[11,12] For example, the pK_a of MO in solutions of tetra(*N*,*N*-dimethyl-*N*-hydroxymethylammonium)-methylentetrapropoxycalix[4]arene decreases by 1.86 logarithmic units due to stabilization of the monoanionic form of the dye.[12]

Stabilization of certain forms of dyes is also observed in their inclusion complexes with calixarenes.[7,8] For example, sulfonatocalix[*n*]arenes (n = 4, 6) forming host−guest complexes with the dye Phenol Blue make it stable at pH 12−13.[7]

Earlier we have shown that macrocycles SCA1 and SCA2 in aqueous solution demonstrate the behavior of surfactants, decreasing the surface tension of solutions in the presence of 64 and 0.89 mM SCA1 and SCA2, respectively.[1] NMR diffusion measurements of the macrocycle SCA2 demonstrated that in 1 mM solutions its number of aggregation is 3. In 10 mM solution, aggregates of SCA2 have head-to-tail packing subunits due to interactions between the substituents of the upper and lower rims of two neighbor molecules with a number of aggregation of 20.[2] Tetraanion macrocycles SCA1 and SCA2 form host−guest complexes with both organic cations (*N*-methylpyridinium, tetramethylammonium (TMA),[13] methyl viologen,[14] and promazine[15]) and neutral molecules (xymedon and dimephosphone[1]). It has been recently demonstrated that cation−radical or neutral species of methyl viologen are stabilized due to their encapsulation into head-to-tail subunits of SCA2 in the electrochemical redox process.[14]

Our present work was aimed at the study of interactions of water-soluble Sulfonatomethylenecalix[4]resorcinarenes SCA1 and SCA2 (Chart 1) with two azo dyes MY and MO known as pH indicators, changing their color upon protonation/deprotonation of their azo group (Scheme 1). The presence of the azo group also enables cis−trans photoisomerization of these dyes, popular nowadays in the preparation of intelligent polymers.[16] Use of pH-dependent dyes in the present work enabled simple and clear visualization of bulky aromatic guest binding by

* To whom correspondence should be addressed. Phone: (007) 843 272 73 94. Fax: (007) 843 273 22 53. E-mail: ella@iopc.ru.

10.1021/jp106060p
Published on Web 09/29/2010

CHART 1: Structure of Water-Soluble Calix[4]resorcinarene Macrocycles and Guest Molecule TMA

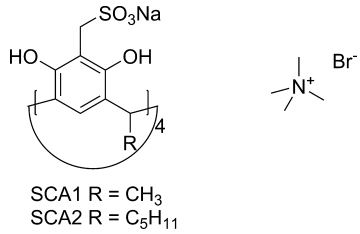

SCHEME 1: Structure and Protonation/Deprotonation Equilibrium of Azo Dyes

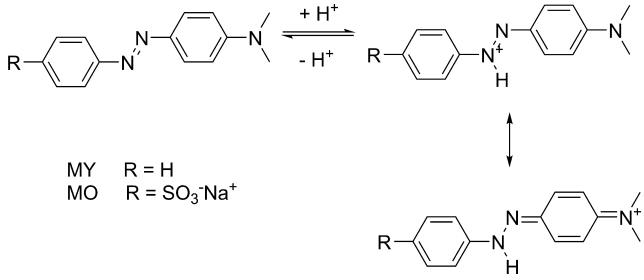

calixarene aggregates. The binding behavior of amphiphilic macrocycle SCA2 was compared with that of its water-soluble homologue SCA1 in aqueous solutions in a monomeric form. Additionally, we considered the interaction of MO−SCA1 and MO−SCA2 complexes with the well-known calixarene substrate TMA.

Experimental Section

Tetramethylenesulfonatocalix[4]resorcinarenes SCA1 and SCA2 were synthesized according to the procedure described earlier in ref 17. MY and MO were from Sigma-Aldrich (Moscow, Russia) and used as received. The purity of dyes was checked by their absorption spectra.

UV−vis spectra were recorded on a Lambda 35 UV−vis Spectrometer (Perkin-Elmer Instruments) using quartz cells with an optical path of 0.2 cm. All spectra were referenced against solvent blanks containing all components except the dyes. The pH of aqueous solutions was measured at 25 °C with a Termo pH meter (Termo Electron Corp.).

All NMR experiments were performed on a Bruker AVANCE-600 spectrometer. The spectrometer was equipped with a Bruker multinuclear *z*-gradient inverse probe head capable of producing gradients with a strength of 50 G cm^{-1}. All experiments were carried out at 303 ± 0.2 K. Chemical shifts (CSs) were reported relative to HDO (4.7 ppm) as an internal standard. The Fourier transform pulsed-gradient spin−echo (FT-PGSE) experiments were performed by a BPP-STE-LED (bipolar pulse pair-stimulated echo-longitudinal eddy current delay) sequence.[18] Data were acquired with a 50.0 ms diffusion delay, with a bipolar gradient pulse duration from 2.2 to 4.8 ms (depending on the system under investigation), 1.1 ms spoil gradient pulse (30%), and 5.0 ms eddy current delay. The bipolar pulse gradient strength was varied incrementally from 0.01 to 0.32 T/m in 16 steps. The temperature was set and controlled at 303 K with a 535 L/h air flow rate in order to avoid any temperature fluctuations owing to sample heating during the magnetic field pulse gradients.

After Fourier transformation and baseline correction, the diffusion dimension was processed with the Bruker Xwinnmr software package (version 3.5). The diffusion experiments were preformed at least three times, and only the data with the correlation coefficients of a natural logarithm of the normalized signal attenuation ($\ln I/I_0$) as a function of the gradient amplitude $b = \gamma^2\delta^2g^2(\Delta - \delta/3)$ (γ is the gyromagnetic ratio, g is the pulsed gradient strength, Δ is the time separation between the pulsed gradients, δ is the duration of the pulse) higher than 0.999 were included. All separated peaks were analyzed, and the average values are presented. The standard deviations of the self-diffusion coefficients determination did not exceed 5%.

2D NOESY experiments were performed with mixing times of 50−400 ms with pulsed filtered gradient techniques. The pulse programs for all NMR experiments were taken from the Bruker software library.

The aggregation numbers of calixarenes are estimated from the simple ratio

$$N_{agr} = V_{agr}/V_{mon} = (D_{free}/D_{sur})^3$$

where V_{agr} and V_{mon} are the volumes of the aggregate and monomer calixarene molecule, respectively, D_{sur} represents the time-averaged self-diffusion coefficient of the calixarene observed in the experiment, and D_{free} is the self-diffusion coefficient of the "free" macrocycle.

To calculate the guest binding fraction (p_b) of a two-site model for the case of fast exchange between the bound and the unbound state of the guest molecule on the NMR time scale the following equation is used[19−21]

$$P_b = (D_{obs} - D_{free})/(D_{complex} - D_{free})$$

where D_{obs} is the apparent (weighed average) self-diffusion coefficient of the guest molecule in the complex, $D_{complex}$ is the self-diffusion coefficient of the complex, and D_{free} is the self-diffusion coefficient of the free guest in the same solvent. $D_{complex}$ is assumed equal to D_{host}, the self-diffusion coefficient of the calixarene.

Solubilization of MY. A 0.0009 g (0.004 mM) amount of MY was added to 4 mL of a solution of SCA1 (5 mM) or SCA2 (0.25, 0.5, 0.75, and 1 mM); the reaction mixtures were kept at room temperature with periodic stirring for 7 days. To separate unsolubilized MY, the mixtures were centrifuged for 15 min (6000 rpm) and the clear supernatant solutions were then used to record the corresponding UV−vis spectra.

Results

Depending on the conditions, three kinds of absorption bands are found to be present in UV−vis spectra of azo dyes, corresponding to both unprotonated (λ_2) and protonated ammonium (λ_1) or to the azonium (λ_3) forms of indicators (for MO its corresponding $\lambda_{2,max} \approx 465$ nm, $\lambda_{1,max} \approx 320$ nm, and $\lambda_{3,max} \approx 510$ nm[22]).

The solubility of MY in water at room temperature is ~6 μM,[23] and the maximum of its absorbance band $\lambda_{2,max}$ is 433 nm (Figure 1, pH 6.2). In the presence of macrocycles SCA1 and SCA2 the solubility of MY in water slightly increases. Depending on the macrocycle concentration, one or two MY absorption peaks ($\lambda_{1,max}$ and $\lambda_{3,max}$) appear in the spectrum (Table 1 and Figure 1).

We studied the pH and number of aggregation (N_{ag}) at different macrocycle concentrations to prove that the appearance of the dye protonated forms is due to them. Aggregation of

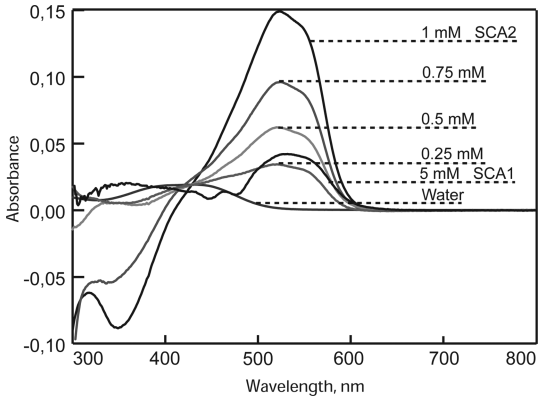

Figure 1. UV−vis spectra of MY in aqueous solutions of SCA1 and SCA2.

TABLE 1: λ_{max}, A, and pH of MY in Aqueous Solutions and Aqueous Solutions of SCA1 and SCA2[a]

C_{SCA1}, mM	C_{SCA2}, mM	λ_1, nm	A_1	λ_2, nm	A_2	λ_3, nm	A_3	pH
0	0			433	0.02			6.2
5.0	0	358	0.02			528	0.04	4.40
0	0.25					520	0.03	6.09
0	0.5					523	0.06	6.06
0	0.75					524	0.10	6.04
0	1.0					523	0.15	6.02

[a] l = 0.2 cm, 25 °C.

TABLE 2: pH and Aggregation Numbers, N_{ag},[a] of Aqueous Solutions of SCA1 and SCA2 at Different Concentrations

	C1		C5	
C, mM	pH	N_{ag}	pH	N_{ag}
10	3.88	1	5.93	20
9	3.88		5.88	
8	3.89		5.92	
7	3.92		5.93	
6	4.02		5.96	
5	4.07	1	5.96	13
4	4.17		5.99	
3	4.27		6.05	
2	4.49		6.09	
1	4.76	1	6.09	3
0.5	5.03		6.21	2

[a] N_{ag} were determined in D_2O solutions.

SCA1 and SCA2 at their different concentrations in aqueous solutions was examined with the FT-PGSE NMR method. Aggregation numbers and corresponding pH of macrocycle solutions are summarized in Table 2. As seen from Table 2, the pH of solutions SCA1 and SCA2 depends on their concentration and varies in the range of 3.88−6.21. Note that for less lipophilic SCA1 this dependence is more pronounced than for SCA2.

The absorbance band $\lambda_{2,max}$ of MO in water is 464 nm (pH 5.7, Figure 2). In the presence of the excess amount of macrocycles SCA1 and SCA2, the absorbance band of nonprotonated form ($\lambda_{2,max}$) is preserved but the position of $\lambda_{2,max}$ shifts relative to its position in water ($\Delta\lambda_2$ = 14 and 6 nm).

SCA1 and SCA2 are sodium salts of tetramethylenesulfonatocalix[4]resorcinarenes; in order to separate the contribution of the ionic strength in the increased solubility of the dyes from the effect of the macrocycles proper, we examined the influence of 100 mM NaCl on the spectra of MO. The $\lambda_{2,max}$ of the absorption band of water-soluble MO at 464 nm was not affected by the ionic strength of its aqueous solution: it did not change even in the presence of 100 mM NaCl.

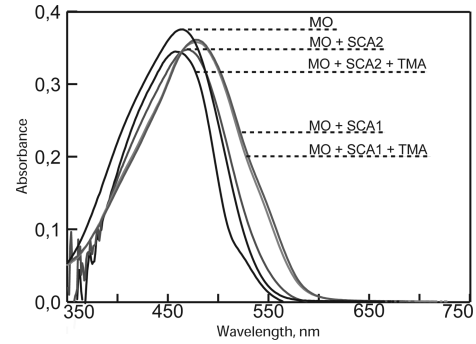

Figure 2. UV−vis spectra of MO (0.074 mM) in aqueous solutions of SCA1 (4.94 mM) and SCA2 (7.41 mM) and in the ternary systems in the presence of TMA (l = 0.2 cm).

Ternary Systems: NMR Study. The strength of the dye−macrocycle complexes and the occupied binding sites were evaluated by their exposure to the well-known guest tetramethylammonium bromide (TMA) bound by SCA1 and SCA2 and their ability to compete for the macrocycle cavity with the MO. It was recently shown that in solutions containing equimolar amounts of SCA2 and TMA (4.5 mM), 91% of TMA is bound in host−guest complexes with the macrocycle.[2]

^{1}H NMR spectra of solutions containing equimolar amounts (1 mM) of macrocycle SCA1 or SCA2 and MO demonstrated a certain difference in their interactions with MO. In the case of macrocycle SCA1, they show a slight downfield shift of the resonance signals of protons of aromatic fragments of the dye (CIS ≈ 0.02 ppm), while for macrocycle SCA2 a slight upfield shift of the signals of the methyl substituents and the aromatic fragment with the amino group of MO were observed (Table 3).

In the presence of a 5-fold excess of SCA1 and a 2.5-fold excess of SCA2 relative to MO, ^{1}H NMR signals of the amino methyl and aryl groups (H^1) of the dye experience an upfield shift.

The ^{1}H NMR PGSE-FT experiment was used to estimate the dimensions of MO in solution and the efficiency of its binding with SCA2 capable of aggregation even in 0.5 mM aqueous solutions. The self-diffusion coefficient, D_s, of MO in the absence of the macrocycle was estimated at two concentrations, 0.5 and 2 mM, resulting in D_s values of 5.88 × 10^{-10} and 5.79 × 10^{-10} m^2/s, respectively. The hydrodynamic radius, $R_{H,}$ of MO was calculated to be 5 Å, and the aggregation number of MO did not change in this concentration range (Table 4). At concentrations above 0.1 mM, MO is known to form dimers that undergo further aggregation in solutions with more than 2 mM MO;[24] thus, the calculated R_H value refers to the dimensions of the MO dimer.

In the presence of a 4.5-fold excess of SCA2 relative to MO, the D_s of the latter decreases to 4.24 × 10^{-10} m^2/s and the hydrodynamic radius of aggregates SCA2-MO increases to 20 Å. The aggregation number of 14 found for SCA2-MO is close to that of individual SCA2 (N_{ag} 13), and the effectiveness of MO binding by SCA2 is 35% (Table 4). 2D NOESY spectra contain only intramolecular cross peaks and indicate no intermolecular interactions between SCA2 and MO.

In solution containing all three compounds, ^{1}H NMR signals of the methyl groups of TMA show a clear upfield shift with CIS $\Delta\delta$ of −1.84 ppm, similar to that in the binary SCA2−TMA system with equimolar amounts of both compounds ($\Delta\delta$ −2 ppm) and corresponding to formation of an inclusion complex

TABLE 3: Chemical Shifts of ^{1}H NMR (δ, ppm) Signals of MO (1 mM) in the Presence and Absence of Macrocycles SCA1 and SCA2

	MO	MO+SCA1 (1:1)	$\Delta\delta^a$	MO+SCA1 (1:5)	$\Delta\delta$	MO+SCA2 (1:1)	$\Delta\delta$	MO+SCA2 (1:2.5)	$\Delta\delta$
NCH_3	3.05 s	3.05 s	0	2.88 br s	−0.17	2.98 s	−0.02	2.73 br s	−0.32
ArH^1	6.90, 6.89 d	6.92, 6.90 d	0.02	6.77 br s	−0.12	6.87−6.86 m[b]	−0.03	6.90−6.86 m[b]	*b*
$ArH^{3,4}$	7.82, 7.81, 7.78, 7.77 q	7.84, 7.83, 7.80, 7.79 q	0.02	7.77, 7.74 br d	−0.04	7.83, 7.81, 7.78, 7.77 q	0	7.77 br s	−0.025
ArH^2	7.91, 7.90 d	7.93, 7.91 d	0.02	7.91, 7.89 br d	0	7.92, 7.90 d	0	7.91, 7.90 br d	0

[a] CIS, $\Delta\delta = \delta_{bound} - \delta_{free}$, where δ_{bound} and δ_{free} are chemical shifts of guest molecules in the presence and absence of the macrocycle. [b] Overlapping signals of SCA2 and MO.

TABLE 4: Self-Diffusion Coefficients (D_s), Aggregation Number (N_{ag}), and Effectiveness of Binding (P_{bD}) for Compounds SCA2, MO, and TMA in D_2O Solutions

System	C_{SCA2}, mM	$D_{s(SCA2)} \times 10^{10}$ m^2/s	C_{MO}, mM	$D_{s(MO)} \times 10^{10}$ m^2/s	$\Delta\delta_{(MO)}$,[a] ppm	C_{TMA}, mM	$D_{s(TMA)} \times 10^{10}$ m^2/s	$\Delta\delta_{(TMA)}$, ppm	N_{ag}	$P_{bD(MO)}$	$P_{bD(TMA)}$
SCA2	4.5	1.40							13		
TMA						4.5	11.7				
SCA2 + TMA	4.5	1.03				4.5	1.95	−2.00	32		91
MO			0.5	5.88					2		
MO			2	5.79					2		
SCA2 + MO	4.5	1.36	1	4.24	−0.34				14	35	
SCA2 + MO + TMA	4.5	1.27	2	4.97	−0.05	3	1.14	−1.84	17	18	100

[a] For $-N(CH_3)_2$ group.

TABLE 5: pK_a, ΔpK_a, λ_{max}, and $\Delta\lambda$ of MO and MY in the Presence and Absence of SCA1 and SCA2 Determined in the Universal Buffer Background

C_{MO}, mM	C_{MY}, mM	C_{SCA1}, mM	C_{SCA2}, mM	pK_a[a]	Δ pK_a	λ_3, nm, pH 2	$\Delta\lambda_3$, nm	λ_2, nm, pH 10	$\Delta\lambda_2$, nm
0.0897	0	0	0	3.25		507		464	
0.0897	0	8.33	0	4.80	1.55	516	9	464	0
0.0897	0	0	8.03	5.15	1.90	514	7	471	7
0	0.08	0	0	3.45		515		447	
0	0.08	8.03	0	4.50	1.05	525	10	465	18
0	0.08	0	8.03	5.35	1.90	526	11	407	−40

[a] $\delta \pm 0.01$.

between SCA2 and TMA. In the same ternary system, signals of the *N*-methyl groups of MO experienced no change (their $\Delta\delta = -0.05$ ppm), while in the binary system SCA2-MO, their CIS $\Delta\delta = -0.34$ ppm and the effectiveness of its binding was 18%. ^{1}H NMR PGSE-FT data also show that the ∼99% binding of TMA in the ternary system (molar ratio of SCA2:MO:TMA = 4.5:3:2) is accompanied by the decrease of the aggregation number of SCA2 to 17, as compared to the binary system SCA2-TMA with $N_{ag} = 32$ (Table 4).

pK_a Values of MO and MY in the Presence of Macrocycles in the Universal Buffer Background. Macrocycle−dye interactions are most pronounced in the change of the protolytic properties of MO and MY, examined in the presence of a 100-fold excess of calixarene in a universal buffer. Under these conditions, macrocycles are capable of binding all available dye molecules fully protonating them. Protonated dyes are bound by the macrocycles not only due to hydrophobic interactions with the aromatic cavity but also due to much stronger Coulomb interactions between the cationic dye and the upper rim of tetraanionic sulfonatomethylencalixaren.

Table 5 shows the pK_a and λ_{max} of azo dyes at different pH values in aqueous solutions in the presence and absence of SCA1 and SCA2 (the different pH values are reached with the help of a universal buffer; $C_{SCA2} = 8.03$ mM, C_{SCA1} 8.33 = mM). The influence of macrocycle−dye interaction on the protolytic properties of the dyes was estimated from titration curves of MO and MY in the presence of a 100-fold excess of macrocycles (Figure 3 shows the absorption spectra for the systems SCA2−MO, SCA1−MO, SCA2−MY, and SCA1−MY as examples).

For water-soluble MO, the transition of solution pH from 2 to 4 in the absence of macrocycles is accompanied by deprotonation and the appearance of $\lambda \approx\sim$ 464 nm instead of $\lambda_{3,max} \approx 510$.

Discussion

Thus, the pH of aqueous solutions of SCA1 and SCA2 depends on their concentration (Table 2, Figure 4). SCA1 behaves like a weak acid, and the increase in its concentration leads to acidification of solution, covering the pH range of 3.88−5.79. As seen from NMR PGSE-FT experiments, at concentrations of SCA2 above 0.1 mM the macrocycle undergoes aggregation. We believe the aggregation of SCA2 is accompanied by the decrease of the macrocycle ionization as compared to SCA1; the increase of the concentration of SCA2 in solution is accompanied by a pH drop from 6.21 to 5.93.

UV−vis spectroscopy studies of interactions of SCA1 and SCA2 with MY demonstrated that water-insoluble MY becomes more soluble in aqueous solutions of the macrocycles and the position of the absorbance depends on the concentration of the macrocycle. The appearance of the $\lambda_{1,max} = 358$ nm band of MY and $\lambda_{3,max} = 528$ nm (at concentration of SCA1 5 mM) and the presence of exclusively $\lambda_{3,max} = 524-528$ nm bands in spectra of solutions containing of SCA2 at concentrations below 1 mM, respectively, correspond to protonation of the amino group of the dye (λ_1) and protonation of the azo group of the dye (λ_3) (Table 1, Figure 1).

On the other hand, in spite of a higher acidity of SCA1 solutions, SCA2 aggregates better solubilized MY than SCA1; the effectiveness of this solubilization is directly proportional to the macrocycle concentration and independent of pH (Table 1). In the absence of the macrocycle at pH 6 MY spectra indicate the presence of only nonprotonated dye (433 nm band).

Thus, it could be suggested that two processes contribute to the solubilization of MY: (1) proton transfer from the macrocycle to the dye and (2) stabilization of the protonated azonium form of the dye upon its binding with the tetraanionic macrocycle. Greater efficiency of the stabilization of the protonated form by SCA2 aggregates ensured a more successful solubilization of MY.

On the contrary, in the UV−vis spectra of water-soluble MO the absorption bands of unprotonated forms, λ_2, remain in the

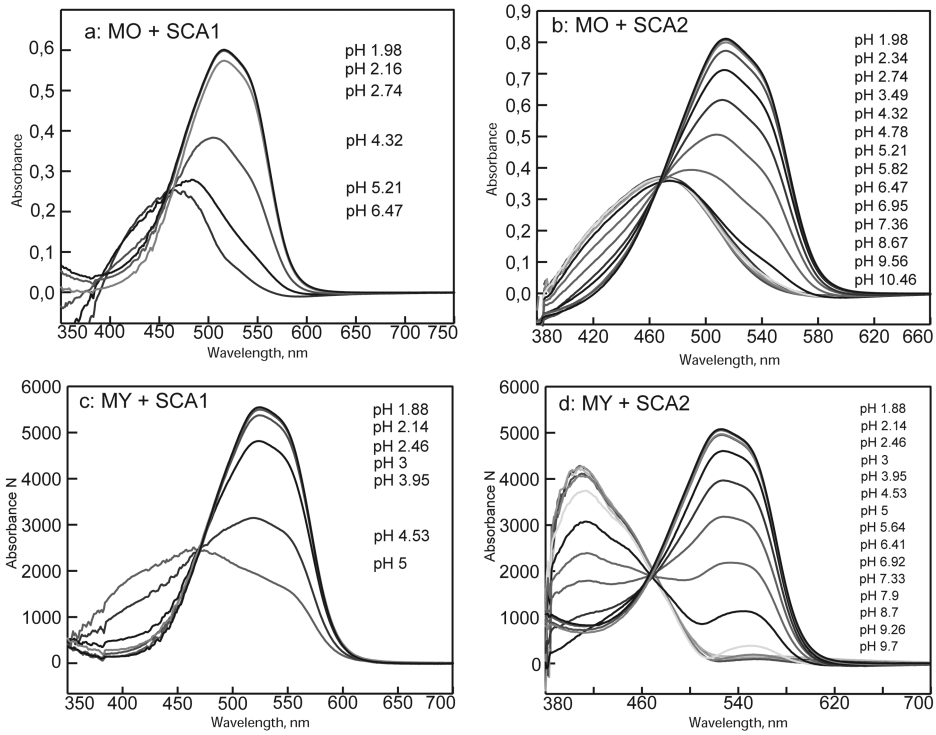

Figure 3. Absorption spectra of MO and MY in the presence of SCA1 and SCA2 at varying pH (universal buffer, $l = 0.2$ cm, $C_{MO} = C_{MY} = 0.08$ mM, $C_{SCA1} = C_{SCA2} = 8$ mM).

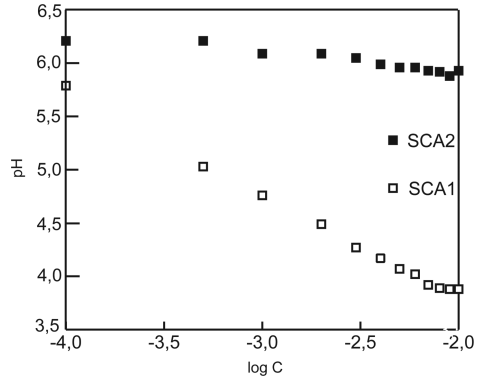

Figure 4. pH values vs the concentration of SCA1 and SCA2.

TABLE 6: λ_{max}, A, and pH of MO in Aqueous Solutions of SCA1 and SCA2 and in the Ternary Systems in the Presence of TMA ($l = 0.2$ cm, 25 °C)

C_{MO}, mM	C_{SCA1}, mM	C_{SCA2}, mM	C_{TMA}, mM	λ_2, nm	A_2	$\Delta\lambda_2$, nm	pH
0.74	0	0	0	464	0.37	0	5.7
0.74	4.94	0	0	478	0.36	14	4.5
0.74	4.94	0	7.51	478	0.35	14	4.5
0.74	0	7.41	0	470	0.35	6	6.7
0.74	0	7.41	7.41	458	0.34	−6	6.6

presence of both SCA1 and SCA2. There are only some shifts (14 and/or 6 nm) as evidence of some interaction. We can assume that part of the MO molecules is also protonated in solutions of the macrocycles, and this is the reason for the bathochromic shifts. MO existing as an anion in these conditions (Table 6) should not be effectively stabilized by interacting with anionic macrocycles and bounded by them.

Interactions of SCA1 and SCA2 with MO at millimolar dye concentrations in the presence of equimolar or less than 10-fold excess of the macrocycle were accessed by ^{1}H NMR spectroscopy. At equimolar macrocycle:dye ratio no CIS in ^{1}H NMR spectra were observed. Formation of inclusion complexes accompanied by CIS of the guest molecule were observed only at macrocycle:dye molar ratios higher than 1:1 (Table 3).

The 2D NOESY spectrum of SCA2 + MO solution contains only intramolecular cross peaks. This fact as well as the small CIS value of MO's protons (Table 3) most likely indicate that MO is bound by the aggregates of SCA2 interacting with their sulphonato groups (Scheme 2). The subunits of head-to-tail packing are retained in the SCA2 aggregates.

The NMR PGSE-FT experiment confirmed formation of associates between SCA2 and MO. Besides, they remain stable upon addition of TMA to their solution, a third component known to form inclusion complexes with this kind of macrocycle. In the ternary system the excess of SCA2 (molar ratio of SCA2:MO:TMA is 4.5:3:2 mM) provides 100% binding of TMA while the rest of the available macrocycle binds the less preferable guest MO. Note that in this case the self-diffusion coefficient (SDC) of the dye is slightly higher than that in a binary SCA2−MO system (Table 4), suggesting the presence of free molecules of MO that are not bound by SCA2 (Scheme 2).

Introduction of competitive guests TMA in macrocycle−dye systems MO−SCA1 or MO−SCA2 causes the appearance of downfield CIS of the proton of MO in ^{1}H NMR spectra. This can be regarded as displacement of MO from the inclusion cavity onto the rim of the cavity or into the bulk of solution (Scheme 2). Unfortunately, a large excess of organic cations and the macrocycles presented in solution does not allow making an unambiguous conclusion regarding the kind of complexes between the dye and the macrocycle, i.e., whether MO forms an inclusion complex or it binds the dye due to the interactions with the upper rim of the cavity.

Interaction of MY and MO with the macrocycles in the presence of universal buffer shifts their acid−base equilibrium due to stabilization of the azonium forms of the dyes. In aqueous solutions in the absence of water-soluble

SCHEME 2: Interaction of MO with the SCA2−TMA System According to FT-PGSE NMR

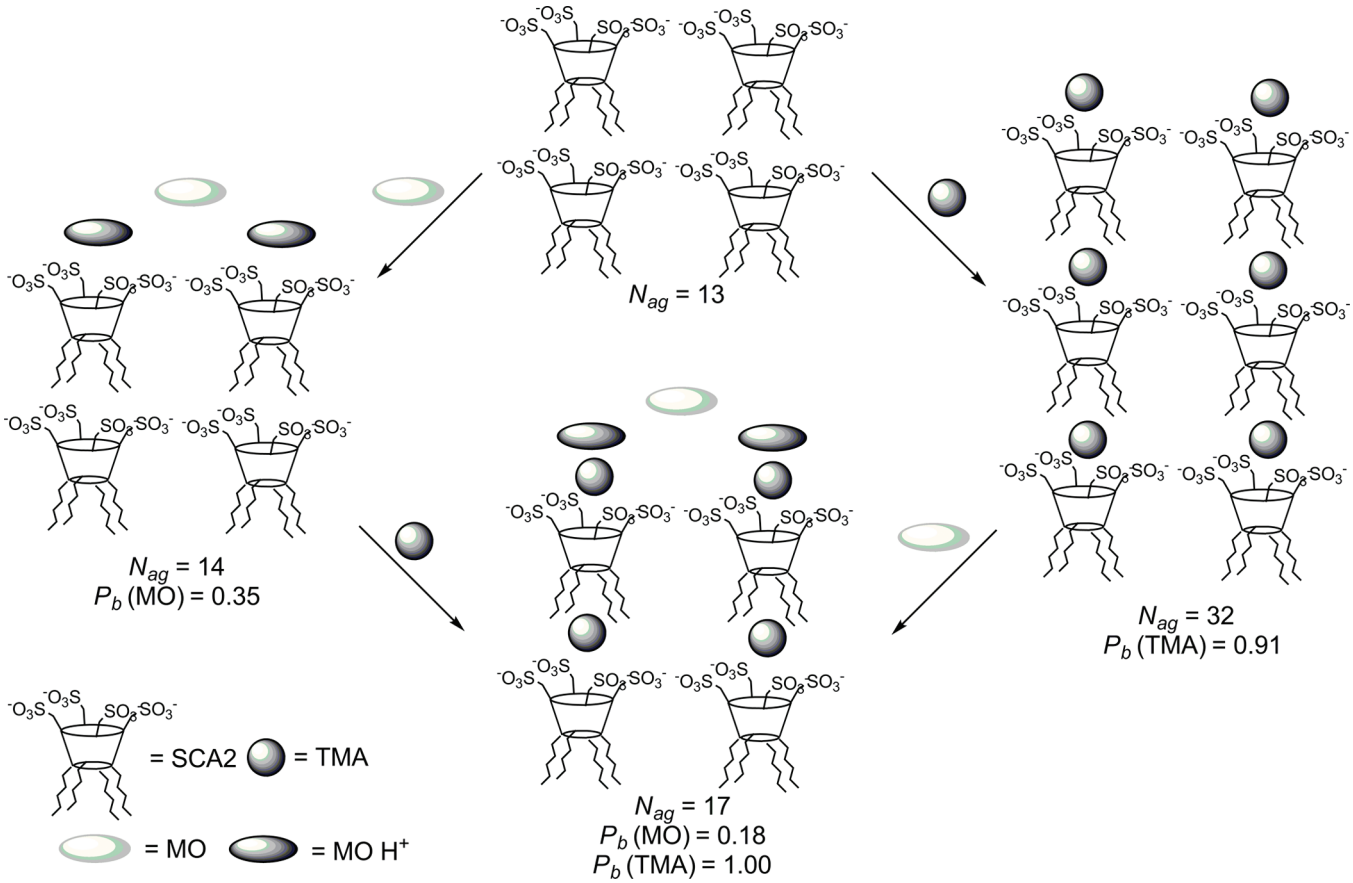

calix[4]resorcinarenes protonated forms of MY and MO exist in the pH range of 2−4, and the corresponding pK_a values are 3.45 ± 0.01 and 3.25 ± 0.01. The presence of the macrocycles in solution extends the range of the presence of protonated MO and MY forms to the neutral pH range: for SCA1 ΔpK_a is about 1.05−1.55. At near-neutral pH the system becomes unstable, and at pH ≈ 7 spectra indicate chemical degradation of the macrocycles (Figure 5).

In the presence of SCA2, the macrocycle−dye system retains its remarkable stability even in basic media (up to pH 10), shifting the acid−base equilibrium of the dye in the same direction; the corresponding ΔpK_a for both dyes is ∼1.90. Thus, unlike monomeric SCA1, binding of azo dyes makes the aggregated SCA2 macrocycle resistant toward the pH change of the media.

The pK_a shift is accompanied by the shift of the absorbance band maxima of protonated ($\lambda_{3,max}$) and nonprotonated ($\lambda_{2,max}$) forms (Table 5). For protonated forms the bathochromic shift of 7−11 nm is similar to those observed for MY and MO in water−alcohol media.[25,26] The latter are related to the dye−solvent interactions affecting the energies of the ground and excited states of the dye molecule.

The bathochromic shift of nonprotonated MY and MO bands ($\lambda_{2,max}$) is presumably related to the presence of the associates with the protonated form of the dye that remains stable even in basic media.

With this in mind, the hypsochromic shift of $\lambda_{2,max}$ of the nonprotonated MY form (−40 nm) in the system SCA2−MY is remarkable (Figure 6). The hypsochromic shift of azo dyes is usually related to the increase of the hydrophobicity of the

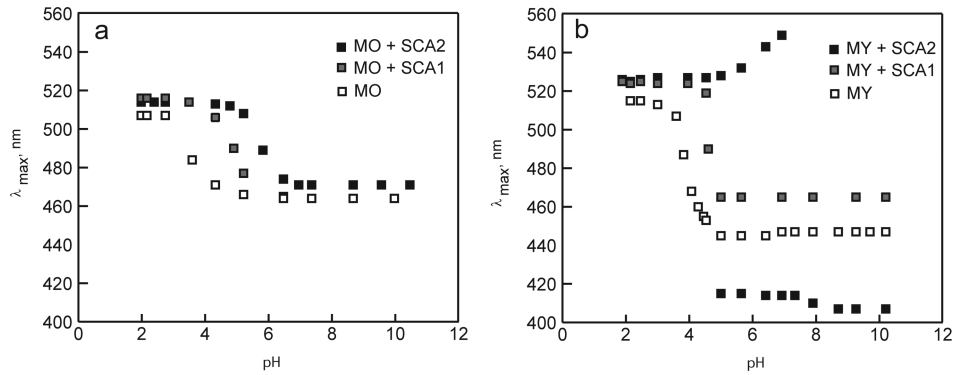

Figure 5. pH dependence of λ_{max} of MO (a) and MY (b) in the absence and presence of macrocycles SCA1 and SCA2 in universal buffer solution (C_{MO} = 0.0897 mM, C_{MY} = 0.08 mM, C_{SCA1} = C_{SCA2} = 8.33 mM).

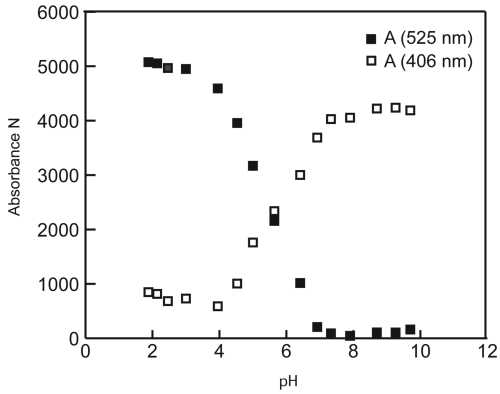

Figure 6. Absorption values of system SCA2−MY.

media.[27] Along with a greater shift of the absorbance maxima, the band is characterized by a relatively high absorbance intensity, close to that of the band corresponding to the azo form of the dye ($\lambda_{3,max}$).

Thus, the nonprotonated form of MY in universal buffer media is effectively stabilized in a strongly hydrophobic environment due to aggregates of SCA2 macrocycles.

Conclusions

In the present paper we reported UV−vis and ^{1}H NMR spectroscopy studies of the interactions of water-soluble tetramethylenesulfonated calix[4]resorcinarenes SCA1 and SCA2 with two azo dyes, MY and MO. Due to the pH-indicator properties of the dyes, it was found that the pH of aqueous solutions of the macrocycles depends on their concentration. It was demonstrated that water-insoluble MY in the presence of SCA1 and SCA2 undergoes solubilization and becomes soluble in their aqueous solutions. Interactions of the azo dyes with the macrocycles are accompanied by their protonation and the appearance of the corresponding bands in UV−vis spectra. A 100-fold excess of the macrocycle stabilizes the azonium form of the dyes. The macrocycle−dye interaction in the universal buffer background shifts the MO and MY protolytic equilibrium ($\Delta pK_{a\ (SCA2)} = 1.90$; $\Delta pK_{a\ (SCA1)} = 1.05-1.55$). Apparently, the macrocycle−dye associates remain stable due to the Coulomb interactions of the cationic fragments of the dye with negatively charged sulfonato groups on the upper rim of the macrocycles. This kind of association does not prevent the aromatic cavity of the macrocycle from involvement in inclusion complexes with such guests as TMA.

Acknowledgment. We would like to thank Dr. Muslinkina for valuable discussion of the results. We wish to thank the Russian Foundation of Basic Research for financial support of this work (RFBR 10-03-00266a).

References and Notes

(1) Morozova, Ju. E.; Kazakova, E. Kh.; Gubanov, E. Ph.; Makarova, N. A.; Archipov, V. P.; Timoshina, T. V.; Idijatullin, Z. Sh.; Habicher, W. D.; Konovalov, A. I. *J. Inclusion Phenom. Macrocyclic Chem.* **2006**, *55*, 173–183.

(2) Syakaev, V. V.; Mustafina, A. R.; Elistratova, Ju. G.; Latypov Sh., K.; Konovalov, A. I. *Supramol.Chem.* **2008**, *20*, 453–460.

(3) Blute, I.; Jansson, M.; Oh, S. G.; Shah, D. O. *J. Am. Oil Chem. Soc.* **1994**, *71*, 41–46.

(4) Fujimoto, T.; Shimizu, C.; Hayashida, O.; Aoyama, Y. *Gazz. Chim. Ital.* **1997**, *127*, 749–752.

(5) Fujimoto, K.; Miyata, T.; Aoyama, Y. *J. Am. Chem. Soc.* **2000**, *122*, 3558–3559.

(6) Shinkai, S. *Calixarenes, a Versatile Class of Macrocyclic Compounds*; Kluwer Academic Publishers: Dordrecht, 1991; pp 173−198.

(7) Tao, W.; Barra, M. *J. Org. Chem.* **2001**, *66*, 2158–2160.

(8) Zhang, Y.; Pham, T. H.; Pena, M. S.; Agbaria, R. A.; Warner, I. M. *Appl. Spectrosc.* **1998**, *52*, 952–957.

(9) Nishida, M.; Ishii, D.; Yoshida, I.; Shinkai, S. *Bull. Chem. Soc. Jpn.* **1997**, *70*, 2131–2140.

(10) Liu, Y.; Han, B.-H.; Chen, Y.-T. *J. Org. Chem.* **2000**, *65*, 6227–6230.

(11) Mchedlov-Petrossyan, N. O.; Vilkova, L. N.; Vodolazkaya, N. A.; Yakubovskaya, A. G.; Rodik, R. V.; Boyko, V. I.; Kalchenko, V. I. *Sensors* **2006**, *6*, 962–977.

(12) Mchedlov-Petrossyan, N. O.; Vodolazkaya, N. A.; Vilkova, L. N.; Soboleva, O. Yu.; Kutuzova, L. V.; Rodik, R. V.; Miroshnichenko, S. I.; Drapaylo, A. B. *J. Mol. Liq.* **2009**, *145*, 197–203.

(13) Mustafina, A. R.; Fedorenko, S. V.; Makarova, N. A.; Kazakova, E. Kh.; Bazhanova, Z. G.; Kataev, V. E.; Konovalov, A. I. *J. Inclusion Phenom. Macrocyclic Chem.* **2001**, *40*, 73–76.

(14) Shalaeva, Ya. V.; Yanilkin, V. V.; Morozova, Yu. E.; Kazakova, E. Kh.; Syakaev, V. V.; Makarova, N. A.; Morozov V., V.; Konovalov, A. I. *Colloid J.* **2010**, *72*, 262–273.

(15) Kazakova, E. Kh.; Syakaev, V. V.; Morozova, Ju. E.; Makarova, N. A.; Muslinkina, L. A.; Evtugyn, G. A.; Konovalov, A. I. *J. Inclusion Phenom. Macrocyclic Chem.* **2007**, *59*, 143–154.

(16) Koshima, H.; Ojima, N.; Uchimoto, H. *J. Am. Chem. Soc.* **2009**, *131*, 6890–6891.

(17) Kazakova, E.Kh.; Makarova, N. A.; Ziganshina, A.Yu.; Muslinkina, L. A.; Muslinkin, A. A.; Habicher, W. D. *Tetrahedron Lett.* **2000**, *41*, 10111–10115.

(18) Neuhaus, D.; Williamson, M. P. *The Nuclear Overhauser Effect in Structural and Conformational Analysis*; Wiley-VCH: New York, 2000.

(19) Cohen, Y.; Avram, L.; Frish, L. *Angew. Chem., Int. Ed. Engl.* **2005**, *44*, 520–554.

(20) Brand, T.; Cabrita, E. J.; Berger, S. *Prog. Nucl. Magn. Reson. Spectrosc.* **2005**, *46*, 159–196.

(21) Pastor, A.; Martinez-Viviente, E. *Coord. Chem. Rev.* **2008**, *252*, 2314–2345.

(22) Oakes, J.; Gratton, P. *J. Chem. Soc., Perkin Trans. 2* **1998**, 2563–2568.

(23) NIOSH. *NIOSH Pocket Guide to Chemical Hazards*: US Department of Health and Human Services, Public Health Service, CDC: Cincinnati, Ohio, 2007.

(24) Kendrick, K. L.; Gilkerson, W. R. *J. Solution Chem.* **1987**, *16*, 257–267.

(25) Fan, J.; Shen, X.; Wang, J. *Anal. Chim. Acta* **1998**, *364*, 275–280.

(26) Fan, J.; Shen, X.; Wang., J. *Talanta* **1999**, *49*, 843–850.

(27) Williamson, Ch. E.; Corwin, A. H. *J. Colloid Interface Sci.* **1972**, *38*, 567–576.

JP106060P